Chapter 3

Plate Radiation Control with Smart Foam

3.1 Introduction

Global radiation control of a simple, baffled monopole source implementing smart foam and an adaptive feedforward controller with a farfield error sensor was successfully demonstrated in the previous chapter. Further experimental studies revealed that considerable farfield sound reduction can be achieved with an error microphone positioned near the source which offers a more compact arrangement. These results provide the foundation for the following experiments which are concerned with plate radiation control i.e. a system with multiple degree of freedom, distributed structural response. An array of smart foam modules is implemented for radiation control of this complex source. A MIMO feedforward Filtered-x LMS controller is used and error signals are provided by microphones in close proximity of the smart foam modules. For a more practical implementation, the reference signal used in the control algorithm is obtained from an accelerometer mounted on the plate surface. The amount of sound power attenuation achieved is compared to the ideal control case which uses a reference

from the signal generator providing the plate excitation. Harmonic and broadband control results are presented. The significance of this research is that it will provide a basis for the implementation of the active/passive smart foam technique to more advanced and realistic noise control problems.

3.2 Experimental Setup

3.2.1 The Noise Source

A clamped, aluminum plate (171 x 149 x 1.5 mm), mounted in a rigid baffle within an anechoic chamber, represents the primary noise source in this experimental study. A schematic of the rear and front surface of the plate is shown in Figure 3.1. A rigid steel baffle borders the front surface of the plate. This simulates the ribbed stiffeners one may find on the fuselage walls of an aircraft. The plate excitation is provided by a PZT actuator (G1195 lead zirconate titanate), measuring 38 x 30 x 0.1 mm, bonded to the rear of the plate. An accelerometer (B&K Type 4374 measuring 6.4 mm in diameter) is also attached to the rear plate surface and acts as an external reference sensor during control in certain experiments. The positions of the piezoelectric actuator and reference sensor were chosen such that the higher order structural modes of the plate could be excited and identified, respectively.

A structural modal analysis, employing laser vibrometer measurements, was performed to identify the modes and corresponding resonant frequencies of the bare plate and of the plate with a homogeneous layer of foam attached to its rear surface. The justification for this analysis is to study the effects of the acoustic foam loading on the system properties and identify the appropriate frequency for active control. The modes and corresponding resonant frequencies for the two configurations are tabulated in Table 3.1. It is noted that the foam loading causes the resonant frequencies of the plate to be shifted lower in frequency which indicates that there is an increase in mass of the system. Active control of the plate radiation was performed between 250 Hz-1000 Hz. In this frequency range, all modes up to and including the (3,3) mode of the plate were excited. Above this frequency range, the sound radiated by the plate may be attenuated solely by

the damping offered by the passive acoustic foam, as observed in the piston radiation control experiments presented in the previous chapter.

(a)

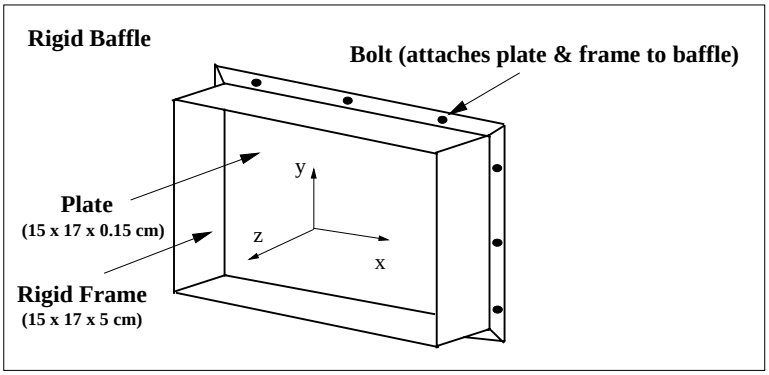

(b)

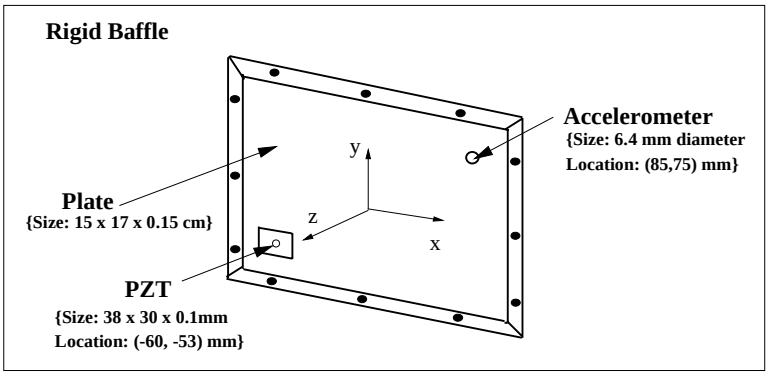

Figure 3.1 (a) Illustration of front of plate. (b) Illustration of rear of plate.

Table 3.1: Comparison of experimental resonant frequencies of bare plate and foam-covered plate.

	MODE	(2,1)	(1,2)	(2,2)	(3,1)	(1,3)	(3,2)	(2,3)	(3,3)
PLATE	Freq. (Hz)	282	310	442	555	610	652	755	973
PLATE & FOAM	Freq. (Hz)	274	302	435	545	559	645	737	933

3.2.2 The Control Actuators

An array of six independent smart foam control modules are used as control actuators in this experiment. Six modules are needed because a MIMO control approach is used implementing a six input/six output configuration. A MIMO control approach is essential for this experiment due to the distributed modal response of the noise source in the frequency range studied. Each smart foam module measures 2.25 x 3.0 x 2.0 inches and consists of a rectangular cube of partially-reticulated polyurethane foam with an embedded PVDF actuator configured as a half-cylinder with a 2.0 inch diameter. As mentioned in the previous chapter, C. Liang et al. [31] showed that the acoustic intensity generated by curved PVDF increases as its diameter increases. As the acoustic intensity of the PVDF actuator is increased, it will exhibit increased control authority over the noise source. Accordingly, the diameter of the PVDF actuator is the largest that can be embedded within the rectangular foam modules used for this plate radiation control application. To promote independent controllability of the multiple smart foam (i.e. prevent cross-coupling during control), a lightweight, rigid wood frame is wrapped around the periphery of each smart foam module. Although a wood frame is used in this application, one could have used a lightweight, rigid composite material. Theory based on the finite element method will be presented in Chapter 4 of this thesis to identify an optimal configuration of smart foam. An illustration of a single smart foam module before and after it is assembled is shown in Figure 3.2(a).

To study the performance of the composite actuator as an acoustic control source, the sound power generated by the actuator was measured with and without the presence of the rigid frame. A single smart foam module is placed in an anechoic environment and driven with approximately 250 volts rms (maximum possible voltage 300 V_{rms}) using broadband random noise $0<f<1600$ Hz. The results are illustrated in Figure 3.2(b) and show that the presence of the rigid frame greatly increases the efficiency of the actuator in the 200 Hz-650 Hz frequency range. In this frequency range, the radiated power is increased by approximately 10 dB. Note that the wood frame restricts the motion of the PVDF actuator in the horizontal direction and creates a “rigid-plane” boundary for the smart foam. As the PVDF vibrates under electrical excitation, the restricted horizontal

displacement translates into an increase in vertical motion of the actuator. Furthermore, in the low-frequency region there is refraction of the radiated sound waves from the PVDF surface which undergo reflection from the wooden frame [37]. As a consequence, more sound output is obtained by the framed smart foam configuration..

(a)

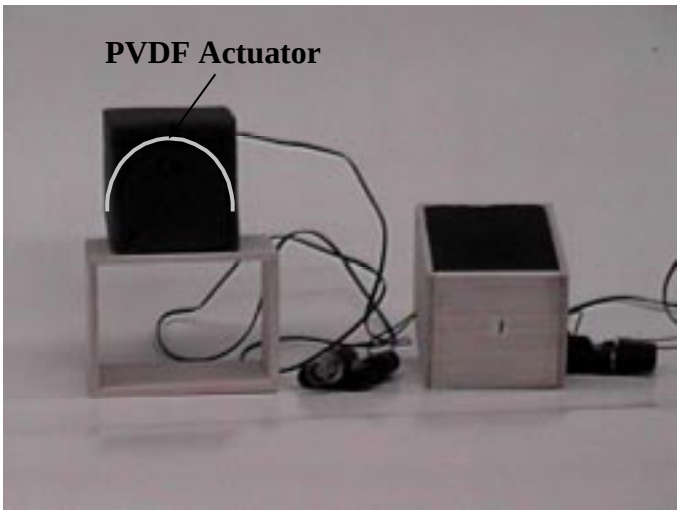

(b)

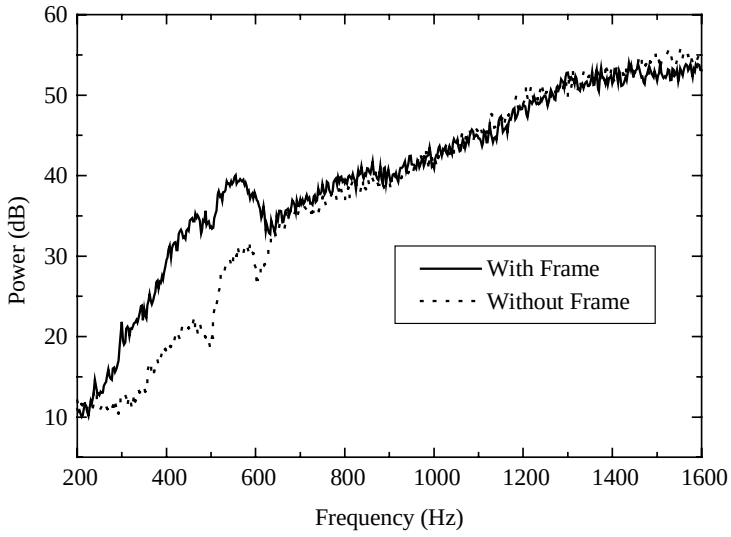

Figure 3.2: (a) Smart foam module. (b) Power radiated by a single smart foam module.

Due to these findings, a frame is placed around each smart foam module for the remaining experiments. The details concerning the power measurement technique used will be explained in a subsequent section

3.2.3 The Error Sensors

The error signals are provided by an array of six PCB piezoelectric microphones located on mounting rods in the nearfield of the control actuators as shown in Figure 3.3. Each error mike is positioned in the center of a smart foam module. The distance of each microphone from its corresponding actuator is easily be changed by adjusting the length of the mounting rods. In the following experiments, the error microphone array location can be changed from a 1.0-9.0 inch distance from the surface of the actuators. The exact location of the error sensor array will be specified as the experimental results are presented.

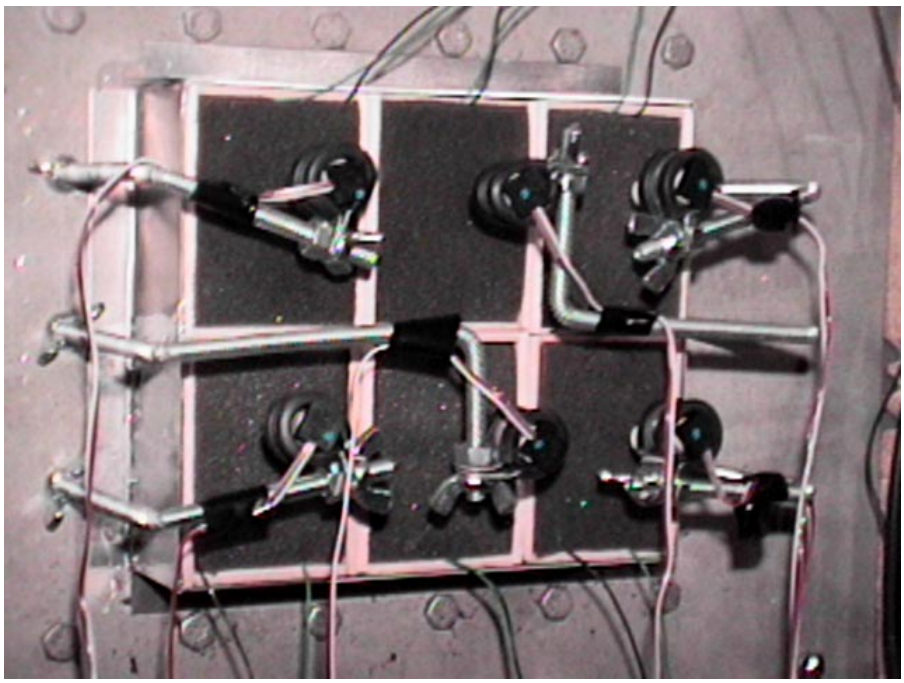

Figure 3.3: Distributed smart foam actuators and error sensor configuration.

3.3 Acoustic Power Measurement Technique

The power measurement procedure [38] involved obtaining the total sound power radiated by the plate before and after control. The radiated power is calculated from the sound pressure levels measured at ten observation microphones mounted on a hemispherical dome or frame as shown in Figure 3.4. The hemispherical frame has a 2.0 ft. radius and is positioned directly in front of the plate. The locations of the observation microphones are such that they measure the sound pressure at points centered on equal areas of the hemisphere. The total acoustic power radiated by the system is determined by the expression:

$$\Pi = \frac{(S/10)}{2\rho_o c_o} \sum_{i=1}^{10} \left| P_i \right|^2 \tag{3.1}$$

where S is the surface area of the hemisphere, P_i represents the sound pressure measured at the i^{th} microphone, ρ_o is the density of air and c_o denotes the speed of sound in air under standard conditions.

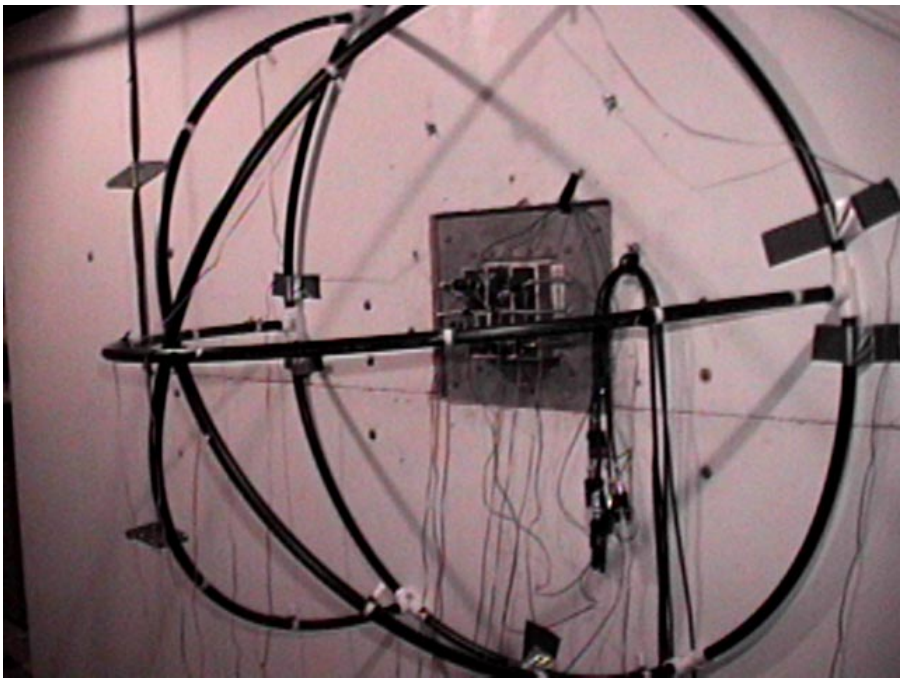

Figure 3.4: Spherical dome for power measurements.

3.4 Experimental Procedure

The plate is mounted inside an anechoic chamber in a rigid baffle. An array of six smart foam modules are mounted directly on the surface of the plate with corresponding error microphones as shown in Figure 3.3. Control of harmonic and broadband sound radiation is studied within a 250 Hz-1000 Hz frequency range. A 6I6O adaptive filtered-x LMS controller is used to establish the appropriate control signal for each smart foam actuator in the array. The control algorithm was implemented with a TMS320C40 DSP board resident in a personal computer. The reference signal is provided by either sampling the excitation signal driving the disturbance piezoelectric actuator (*internal reference*) or by sampling the signal from an accelerometer mounted on the surface of the plate (*external reference*). The radiated sound power of the system is monitored for three different configurations:

(1) the untreated plate (*plate*)

(2) the plate with smart foam modules attached and no control signal applied (*passive*)

(3) the plate with smart foam modules attached and control signal applied (*active/passive*)

For each of these configurations, the sound power level is observed as a function of frequency to indicate the performance of the smart foam noise control treatment. Note that all sound pressure and sound power levels are determined with reference to 20μ Pa and 10^{-12} Watts, respectively.

3.5 *Experimental Results*

3.5.1 *Harmonic Control Results*

Minimization of the sound power radiated by the plate at 545 Hz, which corresponds to the (3,1) structural mode of the bare plate is the goal of the present experiment. Implementing the experimental procedure described above, six independent smart foam modules are positioned on the plate surface. The array of six error microphones are located at a 1.0 inch distance from the surface of the actuators. This location is chosen because a compact arrangement is desired and measurement of cross-radiation between the actuators must be minimized. The 6I6O LMS control code with an internal reference signal is used to attenuate the sound pressure at each error microphone

in the array. Once the error signals are reduced, the sound power is measured for the three system configurations described previously. The active/passive sound reduction at each microphone is illustrated in Figure 3.5(a). This plot indicates there is a 5-15 dB sound reduction at each error microphone, represented by microphone no. 1-6, and a 5-10 dB sound reduction at the observation microphones, represented by microphones no. 7-16. The radiated power is illustrated in Figure 3.5(b) for the same control case. An 8.0 dB attenuation in sound power is contributed by the passive and active control cases, generating a total 16.0 dB active/passive reduction in the radiated power of the plate. Although a slight increase in radiated power occurs at the second harmonic of the drive frequency, due to the nonlinear response of the PVDF actuator, the power level at 1090 Hz remains over 20 dB below the power at the driving frequency during control.

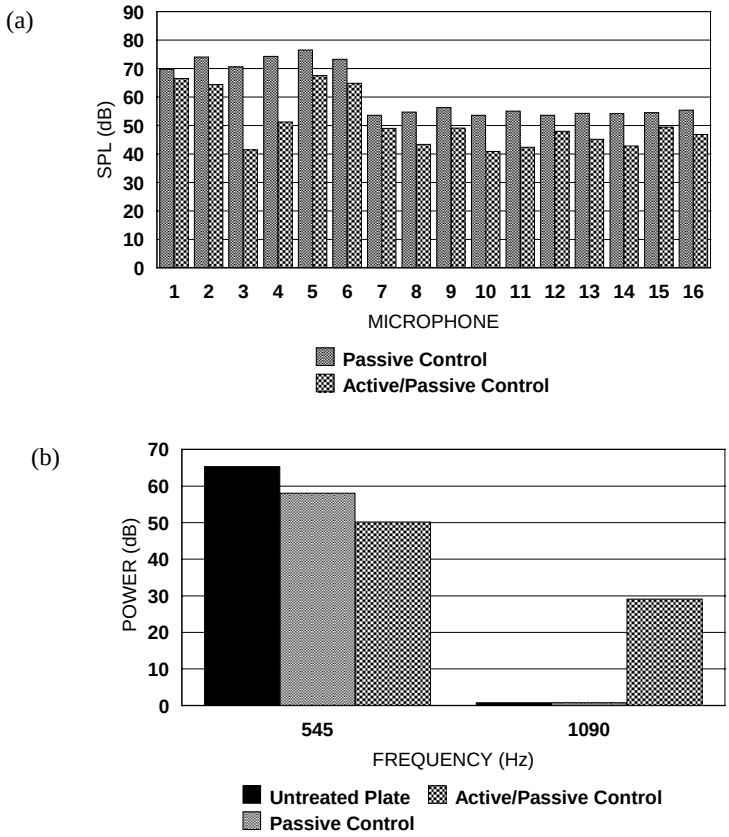

Figure 3.5: (a) Active/passive SPL reduction of (3,1) plate mode at 545 Hz. (b) Active/passive power reduction of (3,1) plate mode at 545 Hz.

3.5.2 *Broadband 1I1O control case with a single smart foam module*

In this experiment, the plate was excited with band-limited random noise 250<f<1600 Hz. Active control is performed up to 1000 Hz allowing the passive sound dissipation of the foam to attenuate the high-frequency sound. To study how the number of smart foam modules used affects the amount of acoustic power attenuation achieved, a single smart foam module was positioned at the center of the plate as shown in Figure 3.6. The remaining exposed area of the plate was covered with a layer of plain, homogeneous foam. A single error microphone was located at a 3.0 inch distance from the actuator surface. This location for the error sensor is comparable to the largest dimension of the smart foam module allowing the sound radiating through the whole surface of the module to be measured. Using a 1I1O LMS control code with an internal reference signal, the pressure is minimized at the error microphone and the radiated sound power is recorded. This experiment is repeated for a 6.0 inch and 9.0 inch error microphone distance. Each error microphone location yielded comparable results in the investigated frequency range.

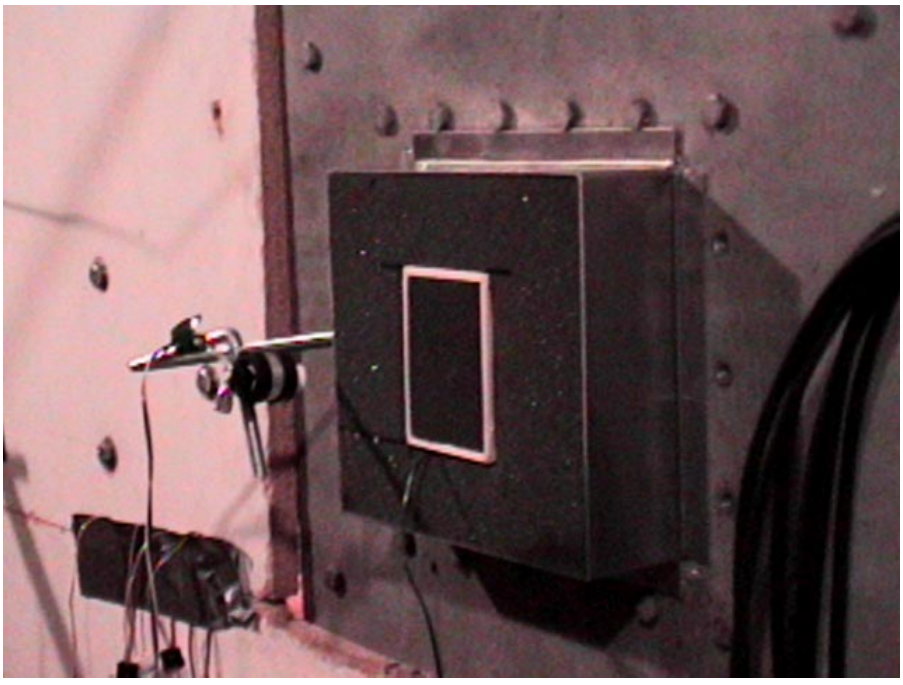

Figure 3.6. Experimental setup for 1I1O broadband control case.

The radiated power before and after control using an error microphone located at a 3.0 inch distance is shown in Figure 3.7. Below 500 Hz, it is observed that the piezoelectric ceramic actuator providing the excitation is unable to generate significant sound output from the untreated plate. As observed in the piston radiation control experiments, the passive smart foam tends to increase the sound output of the foam in the very low-frequency region. This increase in sound output while attempting passive radiation control can be explained in terms of acoustic impedance. Specifically, the low-frequency acoustic resistance (real part of impedance) at the surface of the porous foam layer is greater than that would act on the untreated plate vibrating in the rigid baffle (i.e. there is a radiation coupling between the plate and the passive foam at very low frequencies and the effect is similar to placing a horn in front of the source). The poor active control performance in this low-frequency region is due the low uncontrolled sound levels which overrun the dynamic range of the digital signal processor. Between 500 Hz and 650 Hz, an 8.0 dB passive power reduction is noted at the plate resonance frequencies. Off-resonance, the amount of passive sound reduction is negligible. These observations indicate that in this low-frequency region, the passive smart foam adds structural damping to the system. The addition of active control generates a further 5.0 dB power attenuation over the same frequency bandwidth. Note that satisfactory active control of the plate radiation related to the (3,1) structural mode at 545 Hz and the (1,3) structural mode at 559 Hz is achieved using the single smart foam module in the center of the plate. This is because these are structural modes of the plate covered with passive foam that generate a “monopole-type” radiation patterns. For monopole-type radiators, one active control source can yield satisfactory sound attenuation. Between 650-1000 Hz, about 5.0 dB passive sound attenuation is achieved. A minimal amount of active control is gained due to the increasing complexity of the plate modal response relative to the simple monopole-type radiation pattern offered by the single smart foam actuator. Above 1000 Hz, approximately 10.0 dB passive reduction is achieved and this passive sound reduction is owed to the high-frequency viscous dissipation generated by the passive foam.

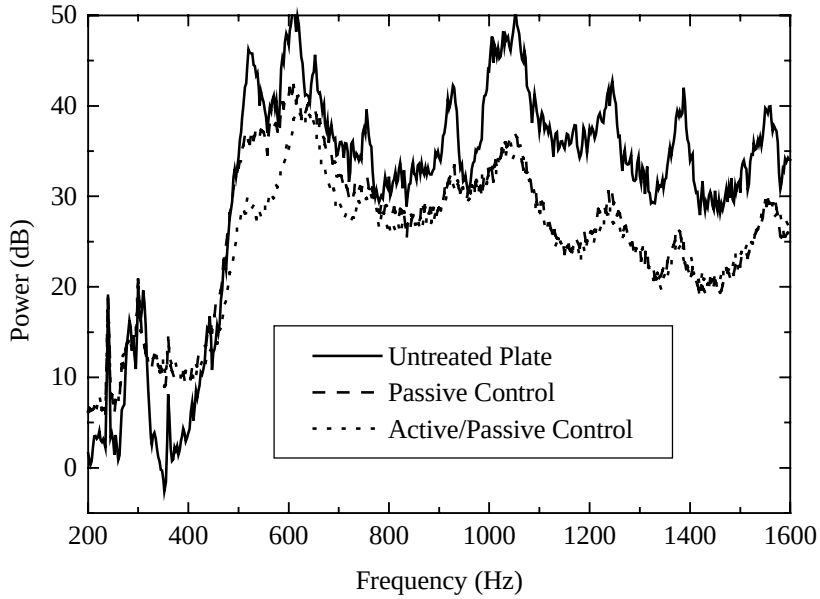

Figure 3.7: Radiated power for broadband 1I1O control case using a single smart foam module.

3.5.3 Broadband 1I1O control case with multiple smart foam modules operating in phase

In this setup, the array of six smart foam modules are connected in phase and used to suppress the broadband sound radiation of the plate. Active control is performed up to 1000 Hz and a single error microphone is located in the center of the array at a 6.0 inch distance from the surface of the actuators. This location corresponds to the largest dimension of the smart foam actuator array which is similar to a monopole type source covering the whole plate surface.

The radiated power before and after control is shown in Figure 3.8 for the 1I1O control case incorporating the array of six smart foam modules. As observed in the previous 1I1O control case implementing a single smart foam module, passive control increases the sound radiation of the system due to a radiation coupling between the acoustic foam and the plate below 500 Hz.. However, the addition of active control reduces the sound power level of the system down to that of the untreated plate. This behavior is attributed to the increase in control authority offered by implementing a distributed active array of smart foam modules over the entire plate surface. Between

500-800 Hz, approximately 5.0 dB passive sound reduction is observed at the plate resonant frequencies and is attributed to the structural damping offered by the foam. Negligible passive sound attenuation is observed at off-resonant frequencies in the same frequency bandwidth. However, the active control case enhances the amount of power attenuation gained by about 5-8 dB. Above 800 Hz, a 10.0 dB passive power attenuation is observed as in the 1I1O single smart foam module control case. In general, for a 1I1O control setup implementing six smart foam modules wired in phase, the active power attenuation of the monopole-type radiating plate modes increases compared to the control performance achieved with a single smart foam module. Distributing an array of smart foam modules over the entire surface of the plate yields an increase in control source strength and explains the improved performance of the present control case.

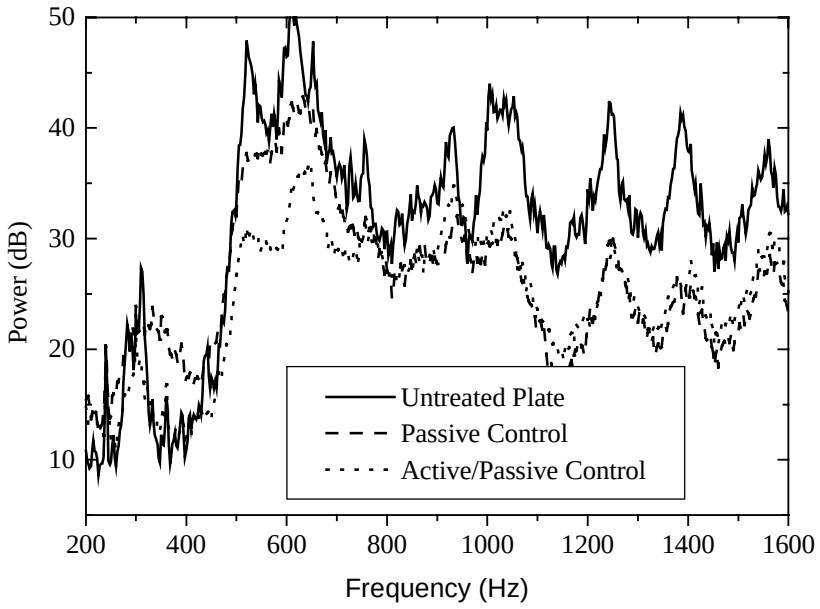

Figure 3.8: Radiated power for broadband 1I1O control case using multiple smart foam modules operating in phase.

3.5.4 Broadband 6I6O control case with multiple, independent smart foam modules

To suppress the broadband radiation of the plate, a 6I6O LMS control code is investigated which allows each of the six smart foam actuators in the array to be driven by an independent control signal. Six error microphones are mounted in front of the smart foam array as illustrated in Figure 3.3, at a 1.0 inch distance from the surface of the actuator array. The radiated power, before and after control, is monitored and two variations of the LMS control code are studied. In the first approach, an internal reference signal (i.e. disturbance signal) is implemented. In the second approach, an external reference signal measured by the accelerometer mounted on the rear surface of the plate is implemented. Although implementing the plate acceleration as a reference represents a more practical control setup, the effect of feedback from the control outputs to the reference signal needs to be canceled. A feedback cancellation filter is designed by sending white noise into the control source prior to startup of the controller. An auxiliary LMS algorithm is used to minimize the difference between the output of the reference detector and the output of the feedback cancellation filter [39].

The results in Figure 3.9 show the average active/passive attenuation at the error microphones (i.e. control cost function) as a function of frequency. The average sound pressure was obtained at each frequency by dividing the sum of the squared pressure values at the error microphones by six (total number of error sensors). The average value is then converted to sound pressure level in dB relative to $20\,\mu Pa$. The results are presented between 250-1000 Hz, since this is the frequency range where active control is performed. As expected, using an internal reference sampled from the signal generator yields the highest attenuation at the error sensors. This observation is owed to good coherence between the reference and the measured error. An approximate 15.0 dB reduction is observed over the studied frequency range. The external reference case provides satisfactory results between 525 Hz and 700 Hz. In this frequency range, using an external reference with feedback removal produces an approximate 10.0 dB reduction at the error sensors. Comparatively, using an external reference without feedback removal only yields about 3.0 dB reduction in the same frequency range.

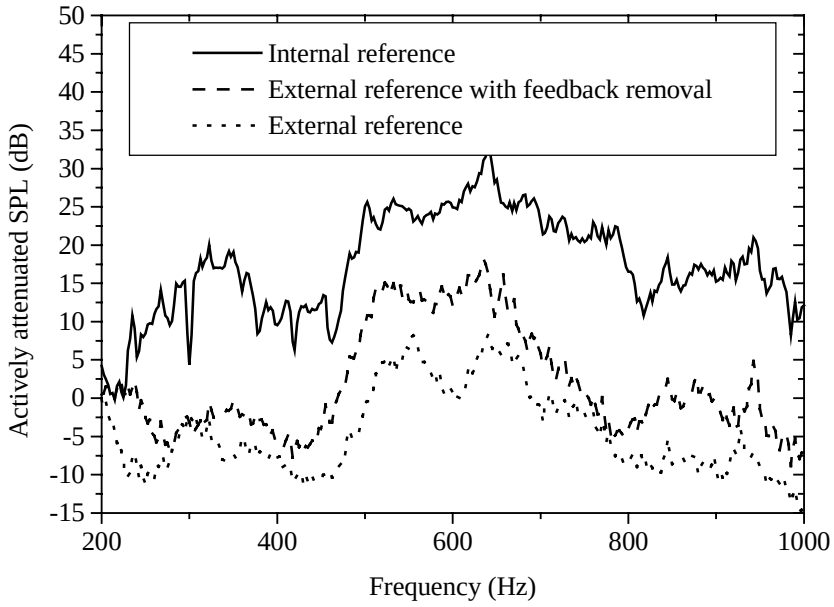

Figure 3.9: Average attenuated SPL at the error microphone array for broadband 6I6O control case using multiple, independent smart foam modules.

These results of Figure 3.9 imply two important facts. Firstly, the plate acceleration can be used as a reference input during control and yields satisfactory sound reduction at the error microphone array, however, the effects of feedback from the control actuators to the reference sensor is not negligible. Secondly, it is observed that the radiation control setup implementing an internal reference sampled from the signal generator yields the highest sound reduction in the studied frequency range compared to the external reference sensor configuration with feedback removal. In the low frequency range, poor coherence is the reason for the lack of active attenuation below 525 Hz when an external reference is used. Above 700 Hz, the poor active control performance occurs because causality becomes an issue due to the higher frequencies of excitation. Causality relates to the travel time delay between the reference sensor and the control output by the secondary control source at the error sensor. To preserve causality of the system, this travel time, which includes the necessary digital control filtering, must be less than the time it takes for the primary source response to reach the error sensor or control cannot be achieved. In the external reference case, the close proximity of the accelerometer to the

smart foam actuators places a narrower time constraint on the response of the digital controller compared to the control scheme that implements an internal reference. This accounts for the satisfactory performance only in a narrow bandwidth (i.e. between 500 Hz-700 Hz) by the external reference sensor compared to the superior broadband performance achieved with an external reference sensor.

The active/passive power attenuation is shown in Figure 3.10 for the 6I6O control case. In Figure 3.10, the control scheme implementing an internal reference yields the highest attenuation of radiated power. About 10.0 dB sound power reduction is observed in the studied frequency bandwidth. The external reference case yields satisfactory results between 525 Hz and 700 Hz. In this frequency range, using an external reference with feedback removal produces an approximate 8.0 dB reduction at the error sensors. Comparatively, using an external reference without feedback removal only yields about 3.0 dB reduction in the same frequency range. As expected, similar trends in power attenuation are observed when compared to the sound reduction achieved at the error sensor array.

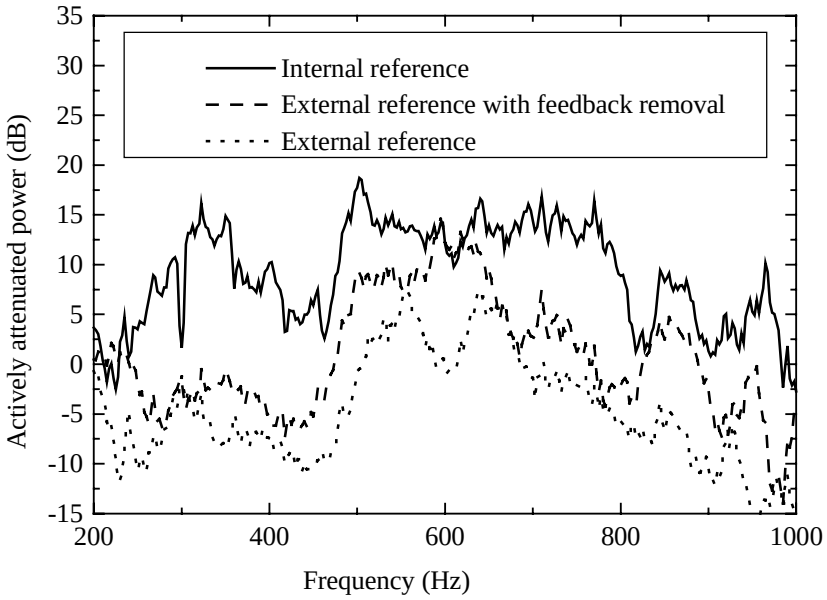

Figure 3.10: Attenuated power for broadband 6I6O case using multiple-independent smart foam modules

Figure 3.11 clearly highlights the potential of smart foam in radiation control applications of complex noise sources. It compares the sound power radiated by the plate with passive and active/passive control, using a 6I6O control scheme with an internal reference. Below 500 Hz, it is observed that the passive foam tends to increase the radiation efficiency of the plate which is an undesirable characteristic. However, the presence of the active component of smart foam reduces the radiated levels below that of the untreated plate. Between 500-1000 Hz, the foam provides approximately 5.0 dB passive sound attenuation at the resonant frequencies. The active component of smart foam provides a further 5-15 dB reduction in the same frequency range. Above 1000 Hz, the passive foam contributes about 10 dB sound power reduction.

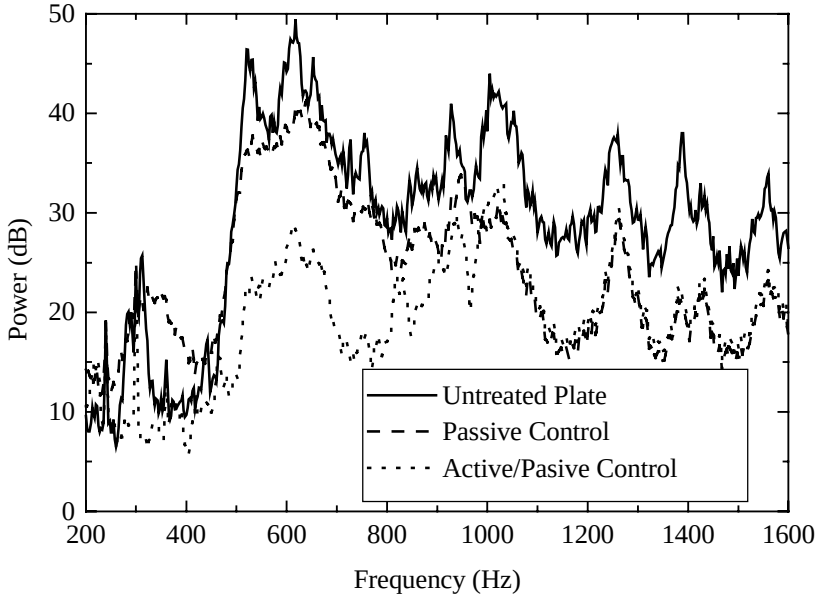

Figure 3.11: Radiated power for broadband 6I6O control case using multiple, independent smart foam modules.

It is interesting to compare Figure 3.11 with the control results of Figure 3.8, where the plate radiation is controlled by a monopole type smart foam configuration (i.e. all the actuators are driven by a single control output and a single error microphone is present). Comparatively, it is observed that an increased sound power reduction is

achieved over a wider frequency range by driving each smart foam actuator independently and minimizing the sound pressure in the nearfield of each actuator. These experiments demonstrate that the physical distribution of the control sources has to be appropriately matched to the primary source modal distribution for significant active sound power attenuation. Specifically, the 6I6O control case implements a six degree of freedom active smart foam distributed over the entire surface of the plate. Considerable broadband active sound power reduction is achieved, compared to the 1I1O control cases, because each smart foam element in the array independently minimizes the radiation generated by the cells that establish the modal vibration pattern of the plate. This multiple degree of freedom approach is necessary for active control in the studied frequency range which contains higher-order plate modes distinguished by cells that vibrate 180^{o} out of phase relative to one another. Accordingly, the radiated power from the complicated source is suppressed by an array of simple monopole control sources with independently adjustable magnitude and phases during control. Corresponding error microphones located in the nearfield of each smart foam control module is sufficient for this collection of monopole type radiators. It is observed that the most appropriate error microphone location corresponds to the largest dimension of the actuator. This permits the error sensor to measure the sound pressure radiated by the entire actuator surface.

3.6 Summary

The potential of the smart foam noise control treatment to suppress the power radiated by a baffled plate has been successfully demonstrated. It offers a compact control arrangement by allowing the control actuators and error sensors to be located in a localized area near the primary source, while producing an overall reduction of the freefield radiated power. Using an internal reference signal, considerable active sound power reduction of random noise was achieved using a 1I1O LMS control code. Comparatively, a 6I6O control setup offered greater active sound attenuation over a wide frequency range. In each configuration, the sound attenuation was further increased due to the passive dissipation offered by the foam, particularly in the high-frequency range. The smart foam performance was also studied using an external reference signal measured by

an accelerometer on the plate. Although the highest power attenuation was achieved by using an internal reference signal and represents the ideal case, implementing an external reference signal provided some attenuation in a narrower bandwidth. The reduced control performance observed when an external reference was implemented can be attributed to poor low frequency coherence and causality issues in the high frequency range. These plate radiation control results indicate that there is some potential for smart foam in more advanced noise control problems.